THE JOURNAL OF BIOLOGICAL CHEMISTRY
Vol. 275, No. 25, Issue of June 23, pp. 19121–19131, 2000

Printed in U.S.A.

Copper(II)-induced Conformational Changes and Protease Resistance in Recombinant and Cellular PrP

EFFECT OF PROTEIN AGE AND DEAMIDATION*

Received for publication, September 13, 1999, and in revised form, March 27, 2000

Kefeng Qin,[a,b] Dun-Sheng Yang,[a] Ying Yang,[c] M. Azhar Chishti,[a] Ling-Jie Meng,[c] Hans A. Kretzschmar,[d] Christopher M. Yip,[e,f,g] Paul E. Fraser,[a,h], and David Westaway[a,i,j]

From the [a]Centre for Research in Neurodegenerative Diseases, the [h]Department of Medical Biophysics, the [i]Department of Laboratory Medicine and Pathobiology, [c]Mass Spectrometry Laboratory, Modern Medicine Research Centre, the [e]Department of Chemical Engineering and Applied Chemistry, [f]Institute of Biomaterials and Biomedical Engineering, and the [g]Department of Biochemistry, University of Toronto, Toronto, Ontario M5S 3H2, Canada, and the [d]Institüt für Neuropathologie, Georg-August-Universität Göttingen, 37075 Göttingen, Germany

While PrP^C rearranges in the area of codons 104–113 to form PrP^{Sc} during prion infections, the events that initiate sporadic Creutzfeldt-Jakob disease are undefined. As Cu(II) is a putative ligand for PrP^C and has been implicated in the pathogenesis of Creutzfeldt-Jakob disease and other neurodegenerative diseases, we investigated the structural effects of binding. Incubation of brain microsomes with Cu(II) generated ~30-kDa proteinase K-resistant PrP. Cu(II) had little effect on fresh recombinant PrP23-231, but aged protein characterized by conversion of Asn-107 to Asp decreased α-helical content by ~30%, increased β-sheet content 100%, formed aggregates, and acquired proteinase K resistance in the presence of Cu(II). These transitions took place without need for acid pH, organic solvents, denaturants, or reducing agents. Since conversion of Asn to Asp proceeds by a spontaneous pathway involving deamidation, our data suggest that covalent variants of PrP^C arising in this manner may, in concert with Cu(II), generate PrP^{Sc}-like species capable of initiating sporadic prion disease.

Prions are infectious pathogens that cause fatal neurodegenerative diseases such as scrapie and Creutzfeldt-Jakob disease (CJD).[1] Many lines of evidence indicate that prions are comprised of an aberrant form of the benign host-encoded neuronal glycoprotein, PrP^C (1). The infectivity-associated isoform of PrP known as PrP^{Sc} differs from PrP^C in several ways including higher β-sheet content and reduced α-helical content (2–5), partial resistance to protease digestion (which yields an N-terminally truncated form denoted PrP27-30 (6, 7)), and reduced detergent solubility. Prion propagation is not thought to involve the replication of a nucleic acid genome but is attributed to PrP^{Sc} molecules templating the refolding of PrP^C to create further PrP^{Sc} molecules, emphasizing the distinction between prions and viruses.

Although the notion of prion diseases as disorders of protein folding is becoming increasingly accepted, many questions remain unanswered. If PrP^{Sc} is the causative infectious agent, why are 10,000–100,000 molecules present per infectious unit? Does this number imply the existence of sub-varieties of PrP^{Sc}? What is the origin of sporadic CJD (sCJD), occurring at a rate of 0.5–1 case per million? This transmissible disease is not attributable to iatrogenic spread or germ line mutation in the human PrP gene (PRNP) and is hypothesized to arise by very rare errors in PrP^C biochemistry that generate PrP^{Sc}-like molecules (8). The nature of these events is obscure, however. Another question raised by sCJD concerns the molecular basis of prion strains. These are distinct isolates of agent with apparently true-breeding attributes that can be propagated in the same inbred host. They are inferred to exist from analyses of the variable neuropathology of sCJD (9, 10) and, more compellingly, from the passage properties of prions isolated from sheep with natural scrapie (11). The existence of strains of scrapie prions was widely interpreted to indicate the presence of a nucleic acid genome (12); however, biochemical analyses have failed to provide strong evidence for such an entity (13). More recent studies indicate that strains are associated with PrP^{Sc} variants that can be distinguished by protease cleavage sites in the vicinity of codon 90 (14, 15) or the accessibility of residues 104–113 to the 3F4 antibody (16, 17). This fits well with the view from molecular genetics, since the gene that controls susceptibility to prion strains, previously referred to as *Prn-i* or *Sinc*, has been found to correspond to a variant allele of the PrP gene (*Prnp*) distinguished by missense changes at codons 108 and 189 (18–21). Nonetheless, the exact molecular distinctions in this region remain to be identified.

PrP^C itself is expressed on the cell surface by virtue of a glycosylphosphatidylinositol anchor. It is composed of an N-terminal domain, which includes reiterated octapeptide motifs of the general form P(H/G)GGGWGQ, and a pathogenesis-associated C-terminal domain that can fold into proteinase-resistant, amyloidogenic aggregates (7, 22). Although its function is debated, a growing body of evidence indicates a role for Cu(II) (23). Binding of Cu(II) to the octapeptide motifs is specific and cooperative (24–27), and cells from PrP gene-ablated ($Prnp^{\%}$)

* This work was supported in part by the Medical Research Council of Canada, Natural Sciences and Engineering Research Council of Canada, the Ontario Research and Development Challenge Fund, the University of Toronto Connaught Fund, Health Canada, the Ontario Mental Health Foundation, and the Alzheimer Society of Ontario. The costs of publication of this article were defrayed in part by the payment of page charges. This article must therefore be hereby marked "*advertisement*" in accordance with 18 U.S.C. Section 1734 solely to indicate this fact.

[b] Supported by a fellowship from the Canadian Red Cross Society.

[j] To whom correspondence should be addressed: University of Toronto, Centre for Research in Neurodegenerative Diseases, Tanz Neuroscience Bldg., 6 Queen's Park Crescent West, Toronto, Ontario M5S 3H2, Canada. Tel.: 416-978-1556; Fax: 416-978-1878; E-mail: david.westaway@utoronto.ca.

[1] The abbreviations used are: CJD, Creutzfeldt-Jakob disease; sCJD, sporadic CJD; PK, proteinase K; DTT, dithiothreitol; MOPS, 4-morpholinepropanesulfonic acid; MALDI-TOF-MS, matrix-assisted laser desorption/ionization time-of flight mass spectrometry; IAM, iodoacetamide; GST, glutathione *S*-transferase; AFM, atomic force microscopy; Tricine, *N*-[2-hydroxy-1,1-bis(hydroxymethyl)ethyl]glycine.

mice have been reported as deficient in membrane-associated Cu(II) (25, 28) and prone to toxic effects of exogenous Cu(II) (29, 30). Possible physiological functions of PrP^{C}-Cu(II) complexes include transport, neuroprotection, or redox enzymatic activity (25, 29, 31). As patterns of protease-resistant PrP fragments characteristic for certain sCJD subtypes can be interconverted via the prior use of metal chelators, it is inferred that PrP^{Sc} is engaged with transition metals in brain homogenates (32) and perhaps *in vivo*.

In this paper we examined structural consequences of metal binding to PrP. The substrates comprised full-length recombinant mouse PrP ("rPrP," MoPrP23-231), which is highly soluble at neutral pH (33), and PrP^{C} isolated from brain homogenates. Our findings reveal a divergence in the behavior of fresh and aged rPrP that is correlated with conversion of Asn-107 to Asp, a modification first described by Sandmeier *et al.* (34), although not previously associated with alterations in structural properties. This covalent change most likely occurs by a well known chemical pathway involving deamidation and hydrolysis. Although studies of a rapid-onset prion disease model found only 0.5 mol % D-aspartyl and L-isoaspartyl residues in PrP^{Sc}, arguing against an obligatory relationship between deamidation and PrP^{Sc} formation (35), our biochemical studies suggest a novel pathway for the formation of PrP^{Sc}-like molecules perhaps germane to the origins of sporadic prion disease.

EXPERIMENTAL PROCEDURES

Recombinant Mouse PrP23-231—Cells of *Escherichia coli* BL2l(DE3) including pRBI-PDI-T7-MoPrP23-231 (pMoPrP23-231) (33) were grown at 37 °C in 1 liter of LB containing ampicillin (100 μg/ml). At $A_{600\ nm}$ = 0.8–1.0, isopropyl-1-thio-β-D-galactopyranoside was added to a final concentration of 1 mM, and the culture was shaken at 37 °C for 16 h. The cells were harvested by centrifugation at 8000 rpm for 10 min, resuspended in 20 ml of suspension buffer (50 mM Tris-HCl, pH 8.0, 1 mM $MgCl_2$, 0.4 mg/ml DNase I, 0.4 mg/ml RNase A, 1 mg/ml lysozme, 1 mM phenylmethylsulfonyl fluoride), and shaken at 37 °C for 2 h and at room temperature for 1 h. The cleared lysate was centrifuged at 4 °C at 39,000 × *g* for 1 h. The insoluble inclusion bodies were washed twice with wash buffer (20 mM Tris-HCl, pH 8.0, 23% sucrose (w/v), 0.5% Triton X-l00 (v/v), 1 mM EDTA, 1 mM benzamidine) and solubilized in 10 ml of 10 mM Tris-HCl, pH 8.0, 50 mM dithiothreitol (DTT), 1 mM EDTA, 8 M urea. After centrifugation at 39,000 × *g* at 22 °C for 1 h, the pH of the supernatant was adjusted to 7.0 with 0.1 mM HCl and applied to an SP-Sepharose column (20 ml, Amersham Pharmacia Biotech) equilibrated with l0 mM MOPS-NaOH, pH 7.0, 5 mM DTT, 1 mM EDTA, 8 M urea, using BioLogic HR chromatography system (Bio-Rad). MoPrP23-231 was eluted with a linear NaCl gradient (0–0.6 M). Fractions containing MoPrP23-231 were pooled and dialyzed against 10 mM MOPS-NaOH, pH 7.0, 5 mM DTT, 1 mM EDTA, 8 M urea, then re-applied to an SP-Sepharose column (20 ml). MoPrP23-231 was eluted with a linear NaCl gradient (0–0.6 M). Pooled fractions containing MoPrP23-231 were diluted with 50 mM Tris-HCl, pH 8.7, 8 M urea to a protein concentration of 0.05 mg/ml. $CuSO_4$ was added to a final concentration of 1 μM, and the solution was stirred for 2 h at room temperature. Oxidation was quenched by addition of 1 mM EDTA, and the pH of the solution was adjusted to 6.5 with 0.1 M HCl. The solution was dialyzed against water, concentrated to 1 mg/ml, and stored at −20 °C. Alternatively, recombinant mouse PrP23-231 (a gift from R. Glockshuber and co-workers) was purified as described previously (33).

Amino Acid Analysis and Determination of Protein Concentration—Amino acid analysis was performed on a Waters PICO-TAG System calibrated in triplicate using a collection of derivatized amino acid standards. Dried MoPrP23-231 was hydrolyzed by a vapor phase using 6 M HCl with 1% phenol at 110 °C for 24 h. After hydrolysis, excess HCl was removed from the hydrolysis tube under vacuum, and the sample was derivatized, dissolved in sample diluent pH (7.4), and an aliquot injected into a Water PICO-TAG column running on a Waters PICO-TAG gradient with a column temperature of 33 °C. For tabulation of individual amino acids, yields are expressed as percentage weight or percentage content with a molecular weight correction for loss of one water molecule per residue.

Mass Spectrometric Molecular Weight Determination and Peptide Mapping—Matrix-assisted laser desorption/ionization time-of-flight mass spectrometric (MALDI-TOF-MS) analyses were carried out using a Perspective Biosystem Voyager-DE STR mass spectrometer (Perspective Biosystems Inc., Farmingham, MA) equipped with a pulsed UV nitrogen laser (337 nm, 3-ns pulse) and a dual microchannel plate detector. For molecular weight determination of full-length MoPrP23-231 protein, spectra were acquired at linear DE mode, acceleration voltage set to 25 kV, grid voltage at 95% of the acceleration voltage, guide wire voltage at 0.150%, delay time at 320 ns, and low mass gate set at 1000 Da; the mass to charge ratio was calibrated with the molecular weight of a mixture of proteins (5734.58 to 16952.56 Da). For analysis of tryptic peptides, the spectra were acquired at reflectron DE mode, acceleration voltage set to 20 kV, grid voltage at 72% of the acceleration voltage, guide wire voltage at 0.050%, delay time at 200 ns, low mass gate set at 250 Da, and the mass to charge ratio was calibrated with the mass of α-cyano-4-hydroxycinnamic acid ($[M + H]^+$ 379.09 Da) and the molecular weight of a mixture of standard peptides (904.46 to 5734.58 Da). Saturated α-cyano-4-hydroxycinnamic acid in 70% acetonitrile containing 0.1% trifluoroacetic acid was used as the matrix for analysis of tryptic peptides, and saturated sinapinic acid in 50% acetonitrile containing 0.1% trifluoroacetic acid was used as the matrix for protein analysis. One microliter of solution of MoPrP23-231 or tryptic peptide mixture was applied on the MALDI plate followed by 1 μl of saturated matrix solution. Spectra were recorded after evaporation of the solvent and processed using GRAMS software for data collection and analysis.

S-Carbamidomethylation of Cysteines—MoPrP23-231 (1 mg/ml) in 50 μl of *S*-carbamidomethylation buffer including 0.1 M Tris-HCl, pH 8.0, 1 mM EDTA, 6 M guanidine hydrochloride was incubated with or without 10 mM DTT at room temperature for 1 h. The reduced or non-reduced MoPrP23-231 was incubated with 50 mM iodoacetamide (IAM) at room temperature in the dark for 30 min. Iodoacetamide reacts with free SH group of cysteine to yield carbamidomethylcysteine. One microliter of MoPrP23-231, reduced or non-reduced MoPrP23-231, treated with IAM was used for MALDI-MS analysis without further purification. Predicted masses were calculated by the Peptide Mass program in ExPASy Home Page.

Measurement of Deamidation via Mass Spectroscopy—Trypsin digestion was carried out with 1 mg/ml MoPrP23-231 (fresh, stored in water at −20 °C for 6 or 24 months) in 10 μl of 100 mM ammonium bicarbonate, pH 8.0, 1 mM $CaCl_2$. 0.5 μl of modified trypsin solution (Sequencing grade, Promega, 2 mg/ml in 50 mM acetic acid) was added to yield a final pH of 7.5 (enzyme:protein = 1:10). After incubation at 37 °C for 2 h, an aliquot (1 μl) of the tryptic peptide mixture was used for MALDI-MS analysis without further purification.

Atomic Force Microscopy—Solution tapping mode atomic force microscopy imaging was performed using a combination contact-tapping mode liquid cell fitted to a Digital Instruments Nanoscope IIIA Multi-Mode scanning probe microscope (Digital Instruments, Santa Barbara, CA). All images were acquired using 120-μm silicon nitride V-shaped cantilevers with integral oxide-sharpened pyramidal tips (type DNP-S, Digital Instruments, Santa Barbara, CA). Prior to use, the AFM tips were exposed to UV irradiation to remove adventitious organic contaminants from the tip surface. The AFM images were acquired using the E scanning head, which has a maximum lateral scan area of 14.6 × 14.6 μm. Optimal tapping mode imaging was achieved at a cantilever drive frequency of ~8.9 kHz with lateral scan rates between 1 and 2 Hz. Under these conditions, the free amplitude of the tip is <3 nm. *In situ* AFM imaging of the mouse PrP protein was achieved by transferring 5 μl of the MoPrP23-231 sample solution onto freshly cleaved mica previously affixed to an AFM sample puck. The sample was immediately sealed in the AFM liquid cell, and the cell was filled with the sample buffer solution. Image analyses were performed using the Nanoscope software version 4.31 (Digital Instruments, Santa Barbara, CA), and NIH Image.

Electron Microscopy—MoPrP23-231 was incubated with 7-fold excess (112 μM) $CuCl_2$, $NiSO_4$, $ZnCl_2$ (or without any divalent ion) at room temperature for 4 days. One-half of each sample was digested with PK (MoPrP:PK = 15:1) at 37 °C for 16 h. For negative staining electron microscopy, 5 μl of each sample was applied to 300-mesh pioloform- and carbon-coated copper grids, blotted dry, and stained with 0.1% phosphotungstic acid, pH 7.0. Samples were then examined under a Hitachi 7000 electron microscope with an accelerating voltage of 75 kV.

Circular Dichroism—Far-UV CD measurements were performed by a JASCO J-715 spectropolarimeter. By using a cell path length of 1 mm, scans were conducted between 190 or 195 and 250 nm at a scan speed of 20 nm/min with a sensitivity of 50 millidegrees. All CD spectrum measurements were performed at room temperature in 25 mM *N*-ethylmorpholine, 30 mM KCl (NEMO-KCl) buffer, pH 7.4, as indicated in the figure legends. To assess the solubility of the protein under these

conditions, aliquots were removed subsequent to each addition of Cu(II) and centrifuged in a Beckman TL100.3 rotor at 45,000 rpm (100,000 × *g*) for 30 min. Supernatants were carefully removed, electrophoresed, and stained with Coomassie Blue. Spectra were subject to curve-smoothing and converted into to [θ] mean residue ellipticities, in degree cm^2/dmol, based on the protein concentration determined by amino acid analysis using the PICO-TAG system.

Peptide Sequencing—MoPrP23-231 was incubated with 7-fold molar excess of $CuCl_2$ for 48 h, digested with PK as above, electrophoresed on a 10–20% Tricine-SDS gel, transferred to a polyvinylidene difluoride membrane, and stained by Coomassie Blue. The membrane was sliced, and individual bands (see text) were sequenced using a Porton Gas-phase Microsequencer model 2090 and on-line phenylthiohydantoin analysis.

Preparation of Brain Microsome Fractions—Subsequent to sacrifice by carbon dioxide inhalation and in accord with the Canadian Council for Animal Care guidelines, brains from Tg(SHaPrP)$7^{+/-}$ heterozygous mice, genotyped by standard methods (36), were removed and immediately frozen on dry ice. Mouse or normal human brain samples were weighed, suspended in 0.32 M sucrose (10% w/v), and homogenized with 6–8 bursts of 10 s each using a Polytron homogenizer set at medium speed. Brain homogenates were then processed to yield microsomes following the method of Meyer *et al.* (37). To aid removal of extraneous proteins, microsomal pellets were suspended in distilled water, incubated for 30 min at room temperature, and then centrifuged at 100,000 × *g* for 1 h at 4 °C (37). The supernatant was discarded, and the pellet was resuspended again in distilled water and stored at −20 °C for further experiments. 40 μl of microsome preparation (at a protein concentration of 0.8 mg/ml) was incubated with or without 140 μM $CuCl_2$, $ZnCl_2$, or $NiSO_4$ at room temperature for 48 h. One-half of each sample was digested with proteinase K (50 μg/ml) at 37 °C for 60 min. The samples were boiled in Tris glycine-SDS gel loading buffer without β-mercaptoethanol and electrophoresed and blotted as indicated.

RESULTS

Disulfide Bond Formation in MoPrP23-231—In initial studies we examined the properties of an N-terminal PrP23-98 fragment of PrP^C used previously for equilibrium dialysis binding studies (25). This peptide yielded a random coil CD signature (as anticipated (38–41)) that was little affected by addition of Cu(II). However, Cu(II) exerted a profound influence on the intact GST/PrP23-98 fusion protein, decreasing the α-helical signature ~3-fold and increasing β-sheet content ~1.5-fold (as determined by standard algorithms (42, 43)). This effect was specific for Cu(II), was not due to aggregation, and was absent from wild-type GST and GST/presenilin 1 fusion protein controls (data not presented). This unexpected finding prompted a study of full-length PrP. For this purpose, recombinant MoPrP23-231 expressed in *E. coli* was purified to homogeneity, by minor modifications to a previously described protocol (33). Of note, oxidation of purified MoPrP23-231 was performed for 2 h at room temperature at a protein concentration of 0.05 mg/ml in 8 M urea at pH 8.7 with 1 μM $CuSO_4$ as a catalyst. After terminating the reaction by addition of 1 mM EDTA, the sample was dialyzed against water to remove urea and thereby promote refolding. MALDI-MS molecular weight analysis of MoPrP23-231 showed a single charged protein signal at m/z 23,108 ± 1.04 Da (Fig. 1, *A1* and *B1*), in excellent agreement with the calculated molecular mass of 23,107 Da as $[M + H]^+$. Mouse PrP contains two Cys residues at positions 178 and 213 (44). To verify that the disulfide bond was present in our recombinant MoPrP23-231, we used the *S*-carbamidomethylation method. After incubation with or without DTT at pH 8.0 in 6 M guanidine hydrochloride, MoPrP23-231 was incubated with iodoacetamide (IAM) and analyzed by MALDI-TOF-MS. Fig. 1*A1* shows that the mass of MoPrP23-231 is 23,109 Da (predicted mass of $[M + H]^+$ is 23,107 Da). Non-reduced MoPrP23-231 did not react with IAM in that its mass did not change (22,099 Da, within the error limits 0.05% for this method of analysis) (Fig. 1*A2*). After reduction with DTT, carbamidomethylated MoPrP23-231 increased in mass by 110–23,209 Da (the predicted gain in mass from two modifications is

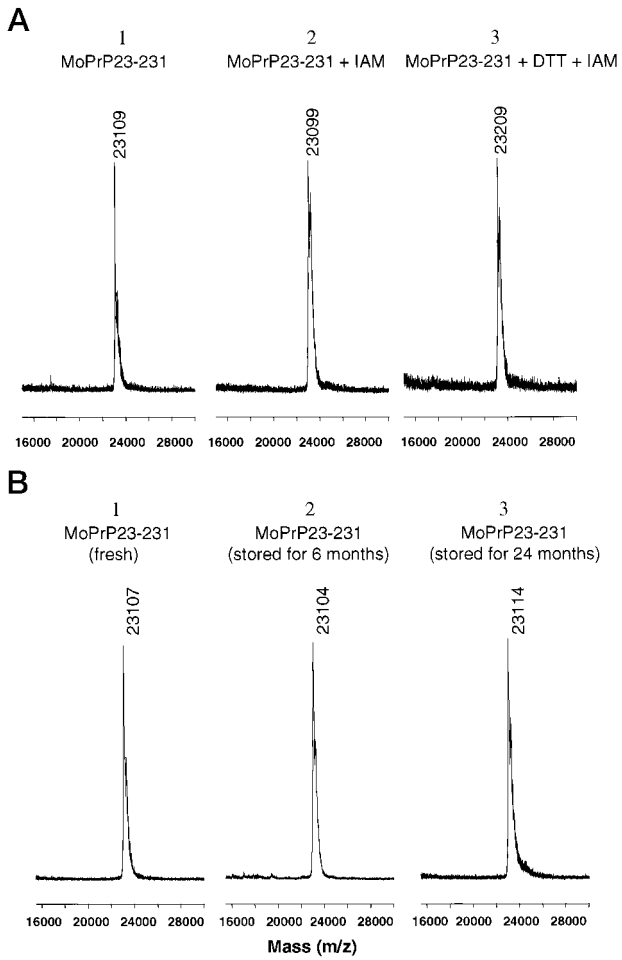

FIG. 1. **MALDI-mass spectra of MoPrP23-231 and determination of a single disulfide bond.** *A, S*-carbamidomethylation of cysteines in freshly purified moPrP23-231. *A1,* MALDI mass spectrum of purified recombinant mouse PrP 23-231 (*MoPrP23-231*). *A2*, mass spectrum of non-reduced MoPrP23-231 incubated with IAM. MoPrP23-231 (1 mg/ml) in 0.1 M Tris-HCl, pH 8.0, 1 mM EDTA, 6 M guanidine hydrochloride was incubated without DTT at room temperature for 1 h. The non-reduced MoPrP23-231 was incubated with 50 mM iodoacetamide (*IAM*) at room temperature in the dark for 30 min. *A3,* mass spectrum of reduced MoPrP23-231 incubated with IAM. MoPrP23-231 (1 mg/ml) in 0.1 M Tris-HCl, pH 8.0, 1 μM EDTA, 6 M guanidine hydrochloride was incubated with 10 μM DTT at room temperature for 1 h. The reduced MoPrP23-231 was incubated with 50 mM IAM at room temperature in the dark for 30 min. *B,* molecular mass of fresh or stored MoPrP23-231. Mass spectra of MoPrP23-231 freshly purified (*B1*), stored in H_2O at −20 °C for 6 months (*B2*), or stored in H_2O for 24 months (*B3*).

114.0 Da and the mass of the di-modified PrP species in the form $[M + H]^+$ is 23,223 Da) (Fig. 1*A3*). These results indicate one disulfide bridge per molecule of the purified MoPrP23-231; they were also verified by detection of a disulfide-bridged peptide fragment subsequent to trypsin digestion of native rPrP (not shown).

Multimeric Forms of Mouse PrP23-231—Purified MoPrP23-231 migrated as a single band with a molecular mass of 23 kDa upon gel electrophoresis, irrespective of whether it was loaded with or without reducing agent (Fig. 2, *lanes 1* and *2*). Negro *et al.* (45) reported that the monomers of reduced and non-reduced recombinant PrP migrated with the same mobility on SDS gels but that the non-reduced protein could form multimers, most probably the result of intermolecular disulfide bond formation. Since a low protein concentration was used here for oxidative refolding (to avoid formation of interchain S–S bonds), the absence of multimers in fresh protein preparations

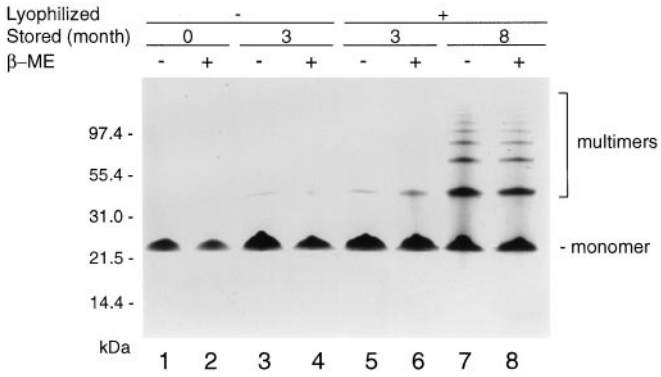

FIG. 2. **PrP23-231 monomers and multimers.** Twenty micrograms of freshly purified, stored, and/or lyophilized MoPrP23-231 in distilled water were electrophoresed on 10–20% Tricine-SDS gel, as indicated, and stained with Coomassie Blue. The molecular weights of the protein markers are indicated to the *left* of the figure. *Even-numbered lanes* represent samples boiled in the presence of β-mercaptoethanol (*β-ME*). Positions of multimers and monomers are shown to the *right side* of the figure.

was not unexpected (Fig. 2, *lanes 1* and *2*). However, aged preparations of MoPrP23-231 examined subsequent to storage (*lanes 3* and *4*) and/or lyophilization (*lanes 5* and *6*) behaved differently and in a manner reminiscent of recombinant chicken PrP (46). For example, fresh MoPrP23-231 (1 mg/ml) in distilled water was lyophilized, stored at −20 °C for 3 months, and then analyzed. After resuspension in the same volume of distilled water, a band corresponding to a putative dimer was detected (Fig. 2, *lanes 5* and *6*). With longer periods of storage, the effect was more pronounced. After lyophilization and storage at −20 °C for 8 months, putative dimers, trimers (~70 kDa), tetramers (~96 kDa), and yet larger oligomers were observed (Fig. 2, *lanes 7* and *8*). This phenomenon was apparent in independent preparations of MoPrP23-231.

To extend this finding, protein preparations were imaged by *in situ* atomic force microscopy (AFM), a technique whereby a sharp tip is raster-scanned over a surface, providing a true three-dimensional image of features at molecular scale resolution. In contrast to traditional imaging techniques, AFM enables examination of biomolecular structures and processes under near-native conditions without the need for exhaustive and possibly damaging sample treatments. By using this approach, freshly prepared MoPrP23-231 revealed well formed, discrete, and comparatively uniform ellipsoid particles with dimensions of 85 ± 14 Å × 100 ± 17 Å × ~19 Å (Fig. 3*A*, and estimated using a standard deviation of ~17% in both lateral dimensions). The ascertainment of lateral dimensions was made after accounting for the known tip convolution effect wherein the shape of the scanning tip contributes to an overestimation of the actual lateral dimensions. Our model, based on a nominal tip diameter of ~20 nm (200 Å), accounts for errors in image analyses and the tip convolution effect (47). Assuming a semi-ellipsoidal shape, a typical protein density of 1.36 Da/Å^3 with a hydration level of ~0.34 g of H_2O/g of protein, and recognizing that the 26-kDa MoPrP23-231 molecules occupies a volume of ~24,600 Å^3, these aggregates are consistent with hexameric MoPrP23-231 species. Notably, somewhat larger particles, ~100 ± 17 Å × ~200 ± 34 Å × ~19 Å in size, were observed in the samples of MoPrP23-231 lyophilized and stored for 8 months. These particles exhibited a propensity to pile up into taller structures (Fig. 3*B, white structures, arrowed*).

Cu(II)-induced Conformational Transitions in MoPrP23-231—A solution of MoPrP23-231 in 25 mM *N*-ethylmorpholine buffer (used to minimize interactions between the buffer and divalent cations (48)) and 30 mM KCl (NEMO-KCl buffer) was examined by far-UV CD (Fig. 4). As anticipated (33), this sample exhibited a CD spectrum indicative of a high α-helical content, with minimum at 208 and 222 nm and a maximum near 195 nm (Fig. 4*A, trace 1*). Addition of excess of Cu(II) failed to produce spectral changes (Fig. 4*A, traces 2* and *3*). Although analysis of MoPrP23-231 stored at −20 °C for 3 months yielded similar results in the absence of cations (Fig. 4*B, trace 1*), addition of 2-, 5-, 7-, and 10-fold molar excess of Cu(II) resulted in a progressive attenuation of the spectral components indicative of α-helical structure and an increment in components indicative of β-sheet plus turn (Fig. 4*B, traces 2–5*). By using the neural net algorithm of Andrade *et al*. (42), at 5× molar excess of Cu(II) α-helix was reduced from 32 ± 2.16 (S.D.) to 22.8 ± 1.0% (n = 4 experiments), and β-sheet was increased from 13.75 ± 1.71 to 26.7 ± 1.7%. Similar data were obtained from a different aged preparation of MoPrP23-231 (Fig. 4*C*, *traces 2–5*); in both cases spectral changes were apparent within minutes of Cu(II) addition. Incubation of the same aged batch of MoPrP23-231 with Ni(II) and Zn(II) failed to produce similar spectral changes (Fig. 4, *D* and *E, traces 2* and *3*). To address the issue of solubility, aliquots of the Cu-MoPrP23-231 preparations analyzed in Fig. 4*C* were removed subsequent to spectroscopic analysis and pelleted at 100,000 × *g* for 30 min. Electrophoretic analysis of the supernatant fraction failed to reveal any appreciable diminution in protein content, making it unlikely that CD spectral changes were due to protein precipitation (not shown).

Cu(II)-induced Formation of Proteinase K-resistant PrP Fragments—In further experiments we investigated another hallmark of PrP^{Sc}, protease resistance, using a preparation of MoPrP23-231 that exhibited Cu(II)-induced CD spectral changes. Protein in NEMO-KCl buffer was incubated with or without 7-fold excess $CuCl_2$ at room temperature for 0, 6, 12, 24, 48 or 96 h at which time one-half of each sample was digested with PK. Bands of monomer (23 kDa) and dimer (46 kDa) were observed in starting material prior to PK treatment (Fig. 5*A, odd-numbered lanes*). Samples mixed with copper and digested directly and those incubated with Cu(II) for a period of 6 h prior to digestion were completely degraded (Fig. 5*A, lanes 6* and *8*), indicating that Cu(II) does not interfere with the PK digestion and is compatible with a previously described sensitivity to protease digestion (33). Incubation of the MoPrP23-231 with Cu(II) for 12, 24, 48, and 96 h resulted in the appearance of two PK-resistant species of ~13.3 and 11.6 kDa (Fig. 5*B, lanes 10, 12, 14*, and *16*). To determine specificity, the same batch of lyophilized protein was resuspended and incubated for 48 h at room temperature with or without 7-fold excess of $CuCl_2$, $ZnCl_2$, $MgCl_2$, $CaCl_2$, $MnCl_2$, $CuSO_4$, $NiSO_4$, or $FeSO_4$ and digested with PK. Only copper (in the chemical form of either $CuCl_2$ or $CuSO_4$) induced formation of PK-resistant PrP fragments. The greater amount of protein concentrations loaded in this experiment allows a third 9.8-kDa species to be detected in addition to the 13.3- and 11.6-kDa peptide fragments (Fig. 5*B*, *lanes 4* and *14*).

The effect of protein "age" was also examined. Freshly purified protein (Fig. 5*C*, *lanes 1, 2, 5,* and *6*) or protein stored for 3 months at −20 °C (Fig. *5C, lanes 3, 4, 7*, and *8*) was incubated alone or with $CuCl_2$ in NEMO-KCl buffer at room temperature for 48 h. Subsequent to electrophoresis, bands of monomer (23 kDa) were observed in all samples without PK treatment (Fig. 5*C, lanes 1, 3, 5*, and *7*). As before, samples incubated without copper and digested with PK were degraded (Fig. 5*C, lanes 2* and *4*). While stored MoPrP23-231 developed PK-resistant forms of apparent molecular mass of 13.3, 11.6, and 9.8 kDa (Fig. 5*C, lane 8*); freshly purified MoPrP23-231 incubated with

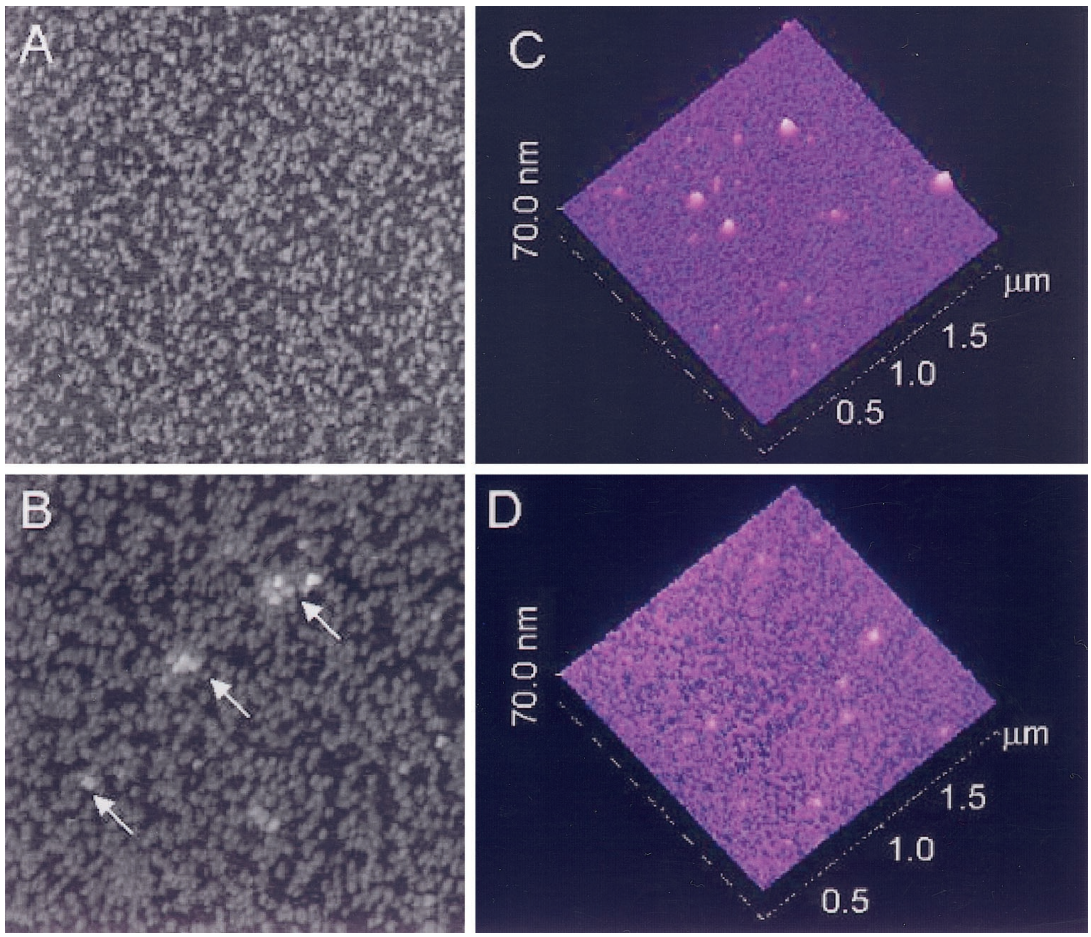

FIG. 3. **Multimeric forms of PrP23-231 detected by atomic force microscopy.** *A* shows freshly prepared MoPrP23-231 analyzed in water, whereas aged MoPrP23-231 (stored for 8 months) analyzed in water is shown in *B*. Image sizes are 1000 × 1000 nm. Sample height is presented on a *gray scale. C* and *D* represent aged MoPrP23-231 (12 months) incubated for 48 h in the presence of Cu(II) (*C*) or Zn(II) (*D*). Increasing sample height is represented by *purple* color, with a side perspective used to visualize the enhanced formation of aggregates in the Cu(II)-treated sample. Aged protein (stored 12 months) incubated in water also contained a small number of aggregates, comparable to the Zn(II)-incubated sample (not shown).

copper was fully digested (Fig. 5*C, lane 6*).

N-terminal Sequencing of Protease-resistant PrP Peptides—Protease-resistant PrP peptides formed in the presence of Cu(II) were subjected to N-terminal sequencing. The 13.3-kDa species corresponds to two approximately equimolar species, consistent with peptides commencing at residues 116 and 118 of mouse PrP (44). The cleavage sites between residues 115 ↓ 116 and 117 ↓ 118 are not identical to those observed when MoPrP23-231 is purified in the absence of protease inhibitors (cleavage at 116 ↓ 117, 118 ↓ 119, and 120 ↓ 121) (33). A less abundant protein species was also present within this size-fractionated sample, and the deduced sequence of T(G)ENFTE aligns with residues 192–199 of mouse PrP (TKGENFTE). Presumably, as protein samples were not treated with reducing agent prior to preparative electrophoresis, a subset of the 13.3-kDa peptide species commencing at residues 116 or 118 are cleaved proximal to residue 192 but fail to dissociate into two parts because of the disulfide linkage between residues 178 and 213. Two attempts to obtain N-terminal sequences from the 11.6-kDa peptide failed to yield a unique sequence but instead yielded weak signals corresponding to peptides present in the 13.3- and 9.8-kDa peptides. Finally, the 9.8-kDa peptide yielded the sequence *S*KKRPKP (where *S* indicates the serine residue inserted to stabilize the protein in *E. coli*) corresponding the to N terminus of recombinant MoPrP23-231 (33). This N-terminal assignment predicts molecular masses of 9605 and 9733.2 Da, assuming C termini defined by residues 115 and 117, respectively, and thereby demonstrates some similarity to chicken PrP fragments detected *in vivo* (49).

Cu(II)-induced Transitions in PrP23-231 Monitored by AFM and EM—Effects of Cu(II) upon the structure of aged preparations of PrP23-231 were also detected by the AFM technique, using Zn(II)-treated samples as controls. It should be noted that AFM signals in Fig. 3, *C* and *D,* are presented as three-dimensional images to emphasize sample height. The most striking feature of this analysis was evident in the Cu(II)-treated samples (Fig. 3*C*), where large and comparatively uniform assemblies of particles were apparent. Thus, whereas the small particles observed by AFM retained an ellipsoidal appearance comparable to that of Fig. 3, *A* and *B*, large aggregated structures were also observed, 500 ± 85 Å wide and extending 120–150 Å off the surface of the mica. These can be seen as "hillocks" in the false three-dimensional perspective (*lighter-colored signals*, Fig. 3*C*). In the case of Zn(II)-treated aged protein samples (Fig. 3*D*), the small (~60 Å tall) particles observed by *in situ* AFM appeared more interconnected in the lateral dimensions than samples prepared in water (not shown) or Cu(II) (Fig. 3*C*), perhaps forming a network on the underlying mica surface. In sum these data suggest that Cu(II) produces a further assembly of MoPrP23-231 complexes (perhaps hexamers, as noted above) to form yet larger supramolecular aggregates.

Since protein preparations enriched in PrP^{Sc} assemble into structures variously termed "prion rods" or "scrapie-associated

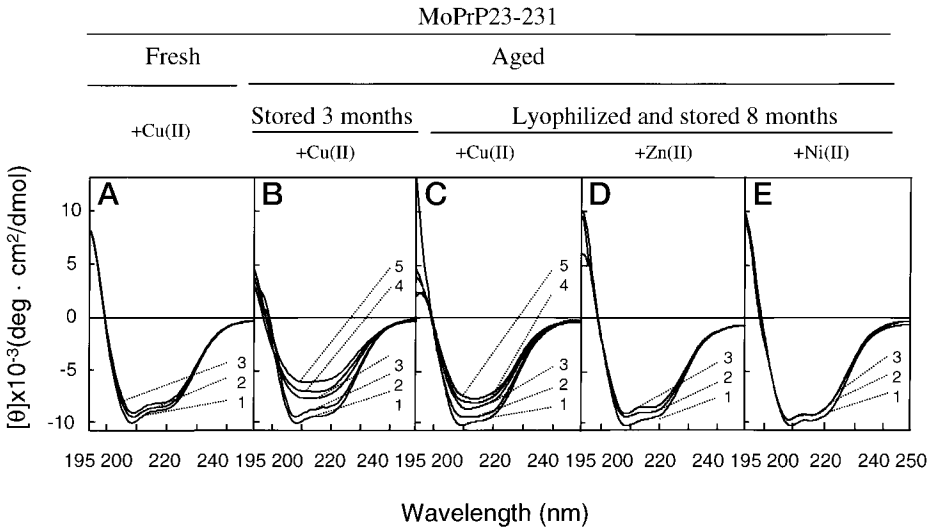

FIG. 4. **Cu(II)-induced conformation transitions in MoPrP23-231.** CD spectra of 10 μM fresh (*A*), stored 3 months (*B*), or lyophilized and stored 8 months (*C–E*) MoPrP23-231 measured in NEMO-KCl buffer, pH 7.4 (*A, trace 1*). Effects of increasing concentrations of Cu(II) (50 and 100 μM) are shown in *A*, *traces 2* and *3*. The effects of increasing concentrations of Cu(II) (20, 50, 70, and 100 μM) are also shown in *B* and *C*, *traces 2–5*, respectively. The effects of increasing concentrations (50 and 100 μM) of Zn^{2+} (*D*) and Ni^{2+} (*E*) are shown in *traces 2* and *3*. The ordinate axis (molar ellipticity [θ]) was calibrated by using a protein concentration determined by amino acid hydrolysis.

fibrils" (50, 51), electron microscopy was also used to investigate the effects of Cu(II) and other metals on ultrastructure (Fig. 6). The preparation of MoPrP23-231 used for experiments shown in Figs. 4 and 5 was incubated alone or with various cations, visualized by negative staining, and observed under the electron microscope. MoPrP23-231 incubated in the absence of divalent cations formed amorphous structures that were eradicated by proteinase digestion (not shown). However, samples incubated in $CuCl_2$ exhibited rod-like structures with a diameter of 20–30 nm and lengths from 200 to 400 nm (Fig. 6*A*). In some instances rod-like structures were assembled together in higher order aggregates (Fig. 6, *B* and *C*). Prion rods show similarities to the Cu(II)-induced fibrils with a diameter of 25 nm and lengths <50 to >300 nm (51), although it should be noted prion rod formation is facilitated by detergent extraction and proteinase K digestion (45) and dependent upon detergent composition (51). After incubation of MoPrP23-231 with Cu(II) and PK digestion, aggregates with a different morphology were observed (Fig. 6, *D–F*), perhaps assemblies of small aggregates and with diameters of 30–40 nm and lengths of 50–100 nm. Parallel incubation of PrP23-231 with Ni(II) or Zn(II) failed to produce any defined morphological structures, either in the absence or presence of proteinase K (not shown).

No Evidence for Methionine Oxidation in Aged MoPrP23-231—Since gel electrophoresis, CD, protease resistance, AFM, and EM techniques all distinguished between fresh and aged MoPrP23-231, we attempted to identify a cause for this phenomenon. Oxidation was a strong candidate as Wong *et al*. (52) have reported that oxidative refolding of recombinant mouse PrP results in selective oxidation of methionine residues. Accordingly, amino acid hydrolysis was performed on two preparations of "aged" MoPrP23-231 that exhibited both Cu(II)-induced CD spectral changes and the formation of PK-resistant species. Analyses are presented for Met, His, Tyr, and Phe (Table I). In no instance was there a progressive reduction in an amino acid content with respect to the predicted yield. As there can be systematic errors in the detection of some amino acid residues subsequent to acid hydrolysis and high pressure liquid chromatography analysis, we also sought post-translational alterations by MALDI-TOF mass spectrometry. Fig. 1*B1* shows the mass of fresh purified MoPrP23-231 is 23,107 Da (predicted mass of $[M + H]^+$ is 23,107 Da). After storage in water at −20 °C for 6 or 24 months, the recorded values are 23,104 or 23,114 Da, respectively (Fig. 1, *B2* and *B3*). The mass differences between three samples (~10 Da) are within the instrument mass error (0.05% of the molecular weight at linear DE mode with the external calibration, corresponding to 11.5 Da for a protein of this size). These results are compatible with those obtained by amino acid analysis and do not support the hypothesis of protein oxidation as a basis for "aging" of MoPrP23-231 (assuming a predicted mass of 23,123 for MoPrP23-231 oxidized to yield 1 mol of methionine sulfoxide per protein molecule and based on values of 149.2 Da for methionine and 165.2 Da for methionine sulfoxide).

Deamidation and Aging of MoPrP23-231—A second possibility for protein aging is via deamidation. These non-enzymatic covalent post-translational modifications occur primarily at asparagine residues, at physiological pH, and through an intramolecular mechanism. Hydrolysis of deamidated residues generates isoaspartate and aspartate (in D- and L- forms) in a ratio of approximately 3:1 (53). Of note, spontaneous deamidation and isomerization of Asn-108 (equivalent to Asn-107 in MoPrP) has been reported in a human PrP106–126 peptide. A molecular audit of MoPrP23-231 revealed the same types of changes at Asn-107, with partial isomerization of Asp-226 also noted (34). We attempted to verify deamidation of Asn-107 to yield isoaspartic acid and aspartic acid using our preparations of aged MoPrP23-231, by exploiting the mass difference of 1 Da between Asn and Asp/iso-Asp. Since this level of resolution is not readily attainable by MALDI-MS (Fig. 1), MoPrP23-231 was analyzed subsequent to endoproteolysis. Because of limiting amounts of aged MoPrP23-231, endoprotease digests were analyzed by MALDI-TOF-MS without a prior high pressure liquid chromatography purification step. A tryptic peptide signal with mass at m/z 501.2 Da was found in all samples analyzed; this corresponds to the protonated peptide YYR (residues 148–150, predicted mass 502.1) and comprises an internal control. In contrast, the fragment 106–109 (TNLK) including Asn-107 exhibited a change in mass. In the freshly purified MoPrP23-231, the TNLK protonated fragment 106–109 had a mass of 475.7 Da (calculated 475.6 Da, Fig. 7, *panel 1*). After storage at −20 °C for 6 months, a second signal of 476.7 Da was observed (Fig. 7, *panel 2*), likely corresponding to TDLK, where D refers to both aspartic and isoaspartic acid residues (which

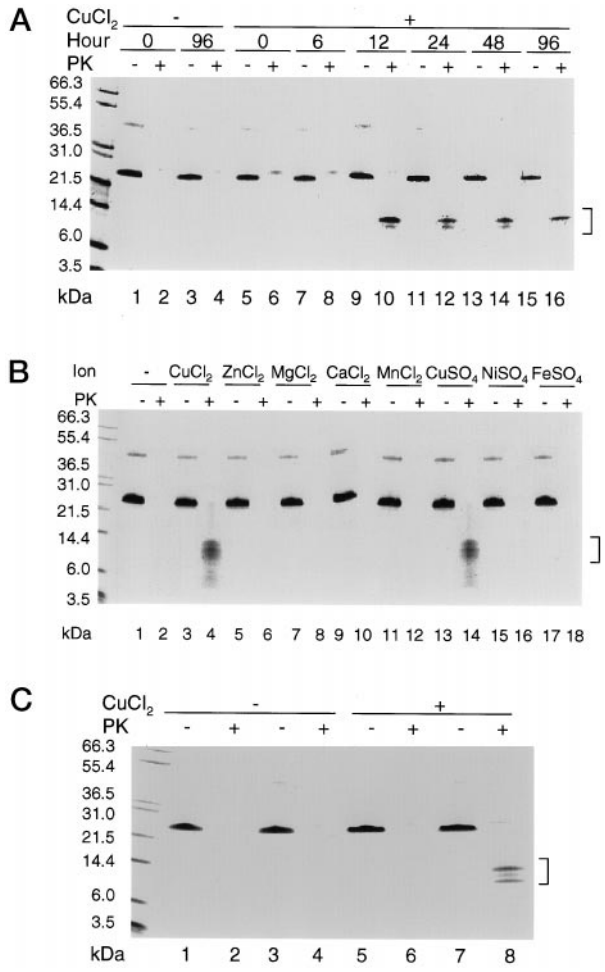

FIG. 5. **Cu(II)-induced formation of protease-resistant fragments of MoPrP23-231.** *A,* time course. An 8 μM solution of MoPrP23-231 (lyophilized, stored for 8 months) in NEMO-KCl buffer, pH 7.4, was incubated without any divalent ion at room temperature for 0 (*lanes 1* and *2*) or 96 h (*lanes 3* and *4*) or with 56 μM $CuCl_2$ at room temperature for 0, 6, 12, 24, 48 or 96 h (*lanes 5–16*). After incubation with or without Cu^{2+}, one-half of each sample was digested with PK (the ratio of MoPrP:PK was 15:1 by mass, equivalent to a PK concentration of 12.5 μg/ml) at 37 °C for 16 h (the *even-numbered lanes*). *Odd-numbered lanes* show samples without PK digestion. The faint band of apparent mobility, 28-kDa, visible in some digested samples corresponds to PK. The position of PK-resistant species is designated by a *bracket* (and also in *B* and *C*). *B,* effect of divalent ions. A 16 μM solution of lyophilized MoPrP23-231 in NEMO-KCl buffer, pH 7.4, was incubated without any divalent ion (*lanes 1* and *2*) or with 128 μM $CuCl_2$ (*lanes 3* and *4*), $ZnCl_2$ (*lanes 5* and *6*), $MgCl_2$ (*lanes 7* and *8*), $CaCl_2$ (*lanes 9* and *10*), $MnCl_2$ (*lanes 11* and *12*), $CuSO_4$ (*lanes 13* and *14*), $NiSO_4$ (*lanes 15* and *16*), or $FeSO_4$ (*lanes 17* and *18*). After incubation with or without divalent ions, one-half of each sample was digested with PK (the ratio of MoPrP:PK was 15:1 by mass, equivalent to a PK concentration of 25 μg/ml) at 37 °C for 16 h (the *even-numbered lanes*). *Odd-numbered lanes* show samples without PK digestion. *C,* effect of protein aging. *Lanes 1, 2, 5,* and *6* represent a fresh preparation, and *lanes 3, 4, 7,* and *8* represent a preparation stored at −20 °C for 3 months. Protein was used at a concentration of 8 μM, with Cu(II) added to a concentration of 50 μM in the *lanes 5–8*. PK was added to a concentration of 12.5 μg/ml and incubated for 16 h at 37 °C as indicated (PrP:PK = 15:1). Proteins were visualized with Coomassie Blue staining of the 10–20% Tricine-SDS polyacrylamide gel.

cannot be distinguished by this type of analysis). After storage for a further 18 months, only the 476.7-Da protonated peptide was detected (Fig. 7, *panel 3*).

Cu(II)-induced Protease-resistant PrP from Brain Microsomes—The foregoing experiments indicate that recombinant MoPrP23-231 characterized by deamidation at residue 107 interacts with Cu(II) to produce molecules with some similarities

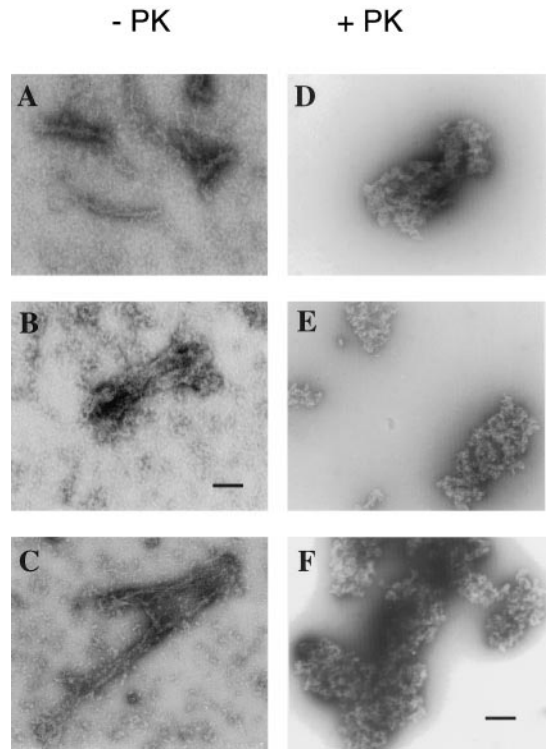

FIG. 6. **Negative stain electron microscopy of Cu(II)-treated MoPrP23-231.** A 16 μM solution of MoPrP23-231 was incubated with 112 μM $CuCl_2$ at room temperature for 4 days. Samples were then digested with PK (the ratio of protein:PK was 15:1 in microgram) at 37 °C for 16 h (*D–F*). *A–C* show the samples without PK digestion. The *size bar* in *B* representing 100 nm also applies to *A*. The *size bar* for *F* represents 200 nm and also applies to *C–E*.

TABLE I
Effect of storage upon amino acid content of MoPrP23–231

Residue	Predicted content of PrP23–231[a]	Observed content in % by frequency (storage time at −20 °C)[b]	
		6 months	12 months
	% by frequency		
Methionine	3.33 (3.97)	3.9 (4.9)	3.5 (4.4)
Histidine	4.29 (5.34)	3.8 (5.1)	4.2 (5.6)
Tyrosine	6.19 (9.18)	5.1 (9.7)	6.3 (11.7)
Phenylalanine	1.43 (1.91)	1.7 (2.5)	1.4 (2.0)

[a] Data in parentheses represent percentage calculated by weight. Fractional amino acid content was calculated taking into account the serine residue inserted prior to codon 23 to facilitate expression in *E. coli* (33). Due to lability during hydrolysis, data for Trp and Cys are not presented.

[b] All MoPrP23–231 preparations examined exhibited Cu(II)-dependent spectral changes by CD and formation of protease-resistant fragments.

to PrP^{Sc}. As discussed below, it is plausible that deamidated forms of PrP^{C} exist in living cells. However, since PrP^{Sc} is formed *in vivo* from post-translationally modified PrP (and consequently bears two *N*-linked carbohydrate side chains itself), we sought to examine the effect of Cu(II) on brain-derived PrP by assaying for protease resistance. Points of particular importance were whether protease-resistant species were formed and, if so, whether the N termini lie in the vicinity of codon 90 (like PrP27–30) or in the vicinity of codons 111 or 117/119/121 (like PrP^{C} and rPrP breakdown products (33, 54)).

These experiments utilized brain microsome preparations containing PrP^{C}, with exogenous Cu(II) added to favor stoichiometric formation of Cu(II)-PrP^{C} complexes. To allow use of the well characterized 3F4 monoclonal antibody (16, 55), analyses were performed upon Syrian hamster (SHa) PrP^{C} expressed in

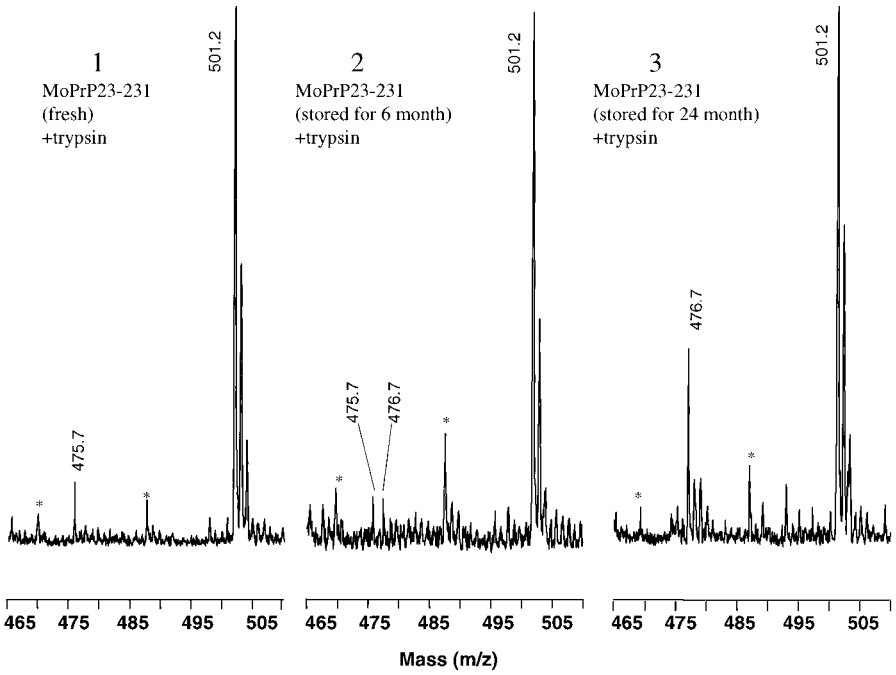

FIG. 7. **Formation of Asp-107 in MoPrP23-231.** Tryptic peptide (residues 106–109 and 148–150) mapping of MoPrP23-231 is shown. MALDI mass spectra of trypsin-digested MoPrP23-231 either freshly purified (*panel 1*), stored in H_2O at −20 °C for 6 months (*panel 2*), or stored in H_2O at −20 °C for 24 months (*panel 3*) are presented here. Peaks labeled with *asterisks* are derived from the matrix.

Tg(SHaPrP7) transgenic mice (36) and PrP^C from normal human brain. Microsomal fractions enriched in PrP^C in NEMO-KCl buffer were incubated with or without transition metals at 140 μM for 48 h, at which time one-half of each sample was digested with PK (50 μg/ml at 37 °C for 1 h). Protein samples were blotted and developed with 3F4 and 6H4 monoclonal antibodies, which recognize epitopes in the vicinity of residues 108–111 and 142–148, respectively (55, 56). These antibodies detect ~30-kDa PK-resistant forms of PrP when microsomes from Tg(SHaPrP)$7^{+/-}$ mice (3F4, Fig. 8*A*; and 6H4, *B*) or human brain (Fig. 8*C*) were incubated for 48 h with Cu(II); such species were completely absent from controls lacking exogenous Cu(II) or containing Zn(II) or Ni(II) (Fig. 8, *A–C, lanes 2, 4,* and *6*). Although attempts were made to use Fe(III) as an additional negative control, this resulted in the formation of precipitates. Addition of Sarkosyl to a final concentration of 0.2% prior to digestion, at a concentration equal to or greater than used by others to detect PrP^{Sc} (7), did not affect the appearance of the PK-resistant species, whereas increasing detergent to 2% abolished their formation (not shown).

The size differences between PK-resistant reactions products from Cu(II)-treated rPrP and microsomal PrP cannot be solely attributed to carbohydrate moieties because an increment of only ~9 kDa distinguishes unglycosylated molecules from diglycosylated PrPc (from apparent mass of 26 kDa for unglycosylated molecules to up to 35 kDa (57, 58)), whereas a difference of >16 kDa distinguishes the largest product deriving from PrP23-231 from the 30-kDa microsomal species. This indicates that the N terminus of microsomally derived PK-resistant PrP must lie upstream of residues 116/118, the termini of the 13.3-kDa fragments from Cu(II)-treated PrP23-231, in agreement with the position of the 3F4 epitope.

DISCUSSION

Cu(II)-induced Changes in rPrP and PrP^C—Although previous studies demonstrate conversion of recombinant PrP to structures enriched in β-sheet structure (one hallmark of PrP^{Sc}), these experiments involve thermal or chemical denaturation, acidification, or reduction of the disulfide bond (26, 59, 60). Similarly, chemical denaturants were also featured in early versions of "conversion" reactions seeded by PrP^{Sc} *in vitro*

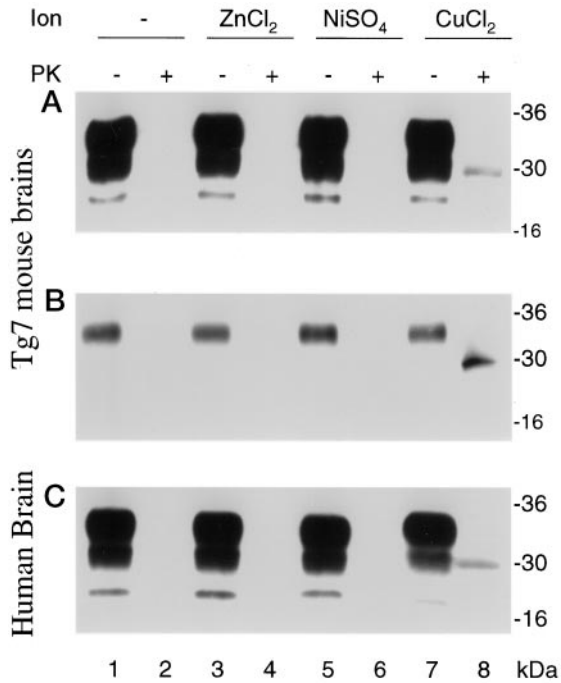

FIG. 8. **Cu(II)-induced protease-resistant PrP from brain microsomes.** 40-μl aliquots of microsomal fraction from $Tg7^+$ mouse brains (*A* and *B*) or human brain (*C*) were incubated without any divalent ion (*lanes 1* and *2*) or with 140 μM $ZnCl_2$ (*lanes 3* and *4*), $NiSO_4$ (*lanes 5* and *6*), or $CuCl_2$ (*lanes 7* and *8*) at room temperature for 48 h. Microsomal preparations presented here were stored between 2 and 3 months at −20 °C prior to gel analysis. One-half of each sample was digested with PK (the ratio of protein:PK was 15:1, equivalent to a PK concentration of 50 μg/ml) at 37 °C for 1 h (*lanes 2, 4, 6,* and *8*). Samples were boiled in the Tris glycine-SDS sample loading buffer without β-mercaptoethanol for 5 min then electrophoresed on a 14% SDS polyacrylamide gel. The proteins were transferred to nitrocellulose membranes and analyzed by Western blot with anti-hamster/anti-human PrP monoclonal antibody 3F4 (*A* and *C*) or anti-mouse PrP monoclonal antibody 6H4 (56) (*B*).

(61, 62), although they have now been superceded (63). PrP27–30-like species have also been created by expression of mammalian PrP in the yeast cytoplasm or under conditions where

disulfide bond formation and *N*-glycosylation is attenuated in chemically treated neuroblastoma cells (64, 65). To what extent some of the more drastic manipulations listed above approximate conditions in living cells is unclear. Our studies demonstrate effects of Cu(II) on the architecture of prion protein molecules, measured in terms of aggregation state, secondary structure, and protease resistance, at neutral pH and in the absence of denaturants and reducing agents. Zn(II), although also capable of coordination by histidine residues, failed to induce equivalent transitions in any of the experiments, with between one and five other transition metals comprising additional negative controls, depending upon the particular paradigm. These data confirm the specific interaction between PrP and Cu(II) (26). Interestingly, Cu(II) has also been shown to affect multimerization of α-synuclein, a protein implicated in the pathogenesis of Parkinson's disease (66).

Covalent Changes in Aged MoPrP23-231—One unanticipated aspect of our experiments was the profound effect of aging on rPrP (MoPrP23-231) produced by a standard method of refolding under oxidative conditions (33, 56, 67). Similar to studies of hamster PrP29-231 (26), Cu(II) has little effect upon the far-UV CD spectrum of freshly prepared MoPrP23-231 when analyzed at room temperature. However, aged preparations exhibit profound changes in the presence of Cu(II) without recourse to thermal denaturation (26) and acquire, with kinetics in the order of hours, resistance to proteinase K. Aged preparations of PrP23-231 also have a propensity to assemble into multimeric aggregates, detected in denaturing polyacrylamide gels and by atomic force and electron microscopy. The practical implication of this finding is that shelf life must be factored as a variable in studies using rPrP.

Oxidative modification of amino acids containing a sulfur atom or an aromatic ring was considered as a mechanism for protein aging, as this may lead to increased exposure of hydrophobic aspects of the protein, favoring aggregation and protease resistance (68). However, amino acid analysis of four of the amino acid residues particularly susceptible to oxidation failed to reveal progressive under-representation with increasing storage times (Table I). Likewise, analysis by MALDI-MS failed to reveal an increase in multiples of 16 mass units between freshly purified MoPrP23-231 and protein stored for 6 or 24 months (Fig. 1*B*). Deamidation of Asn to form aspartic or isoaspartic acid residues, a reaction that proceeds by an intramolecular reaction at neutral pH and can alter the structural integrity and biological activity of proteins, was considered as another possibility (69–71). Sandmeier *et al.* (34) recently reported that Asn-108 in the human PrP peptide 106–126 and the equivalent residue in MoPrP23-231 (Asn-107) undergoes spontaneous deamidation to produce aspartic or isoaspartic acid residues. This is compatible with our knowledge of PrP, since while rates of deamidation can be impeded by secondary structural elements (72), Asn-107 lies within a region with no assigned structure (40, 41). We used MALDI-MS to confirm the presence of Asp-107 in our preparations of MoPrP23-231 by analyzing the tryptic peptide 106–109, TNLK. The TNLK signal was accompanied by a TDLK peptide 1 mass unit heavier (Fig. 7) in material stored for 6 months, and in material stored for 24 months the progenitor TNLK peptide was no longer detectable. In addition to the presence of TDLK peptide paralleling progressive alterations in the properties of stored mouse PrP (documented in Figs. 2–6), chemical changes produced by deamidation and isomerization appear plausible on structural grounds as a basis for changes in the properties of MoPrP23-231. First, Asn-107 is highly conserved, being present in the PRNP gene of chickens and in nearly all mammalian species (73), including humans and sheep, that are susceptible to natural prion diseases. It lies in the center of a "conformationally plastic" region that undergoes extensive remodeling in PrP^{Sc} and may include an alternative transmembrane domain (74, 75). Second, deamidation by virtue of the creation of aspartic acid and/or isoaspartic acid is predicted to generate a change in charge and a side chain capable (at least in other proteins) of coordinating Cu(II). It will be of interest to test the hypothesis that deamidation-related covalent changes compromise the crucial difference between fresh and aged rPrP, using site-directed mutagenesis in the vicinity of Asn-107.

Asparagine Modification, Cu(II), and Prion Protein Biology—The synergism between Cu(II) and aged, deamidated PrP prompts a number of questions. What are the precedents for Asn modification *in vivo*? Are there indications that PrP^{C} is modified in this way, and if so, how might modifications be involved in the physiology and pathobiology of prion proteins? In fact, there is evidence for deamidation and isoaspartate formation *in vivo* in proteins such as hemoglobin and crystallin (76, 77) and in the paired helical filaments of Alzheimer's disease, which are comprised of the microtubule-associated protein tau (78). Strikingly, recent findings on G-coupled proteins indicate that conversion of Asn to Asp may be required to generate abundant forms of these enzymes and modulate biological activity (79, 80). With regard to PrP^{C}, it is interesting to note that deamidation is a spontaneous intramolecular reaction that proceeds at neutral pH. For PrP23-231, the half-life for conversion of Asn-107 to isoaspartic acid is about 30 days (34). Assuming a typical lifetime of 5 h for a PrP^{C} molecule (2) and no competing editing processes (since the repair enzyme protein L-isoaspartylmethyltransferase is only known in cytosolic and endoplasmic reticulum-retained incarnations (81, 82)), a small fraction of PrP^{C} molecules might be predicted to be modified spontaneously at Asn-107 and perhaps at other sites. Since there are suggestions of mammalian deamidases expressed in the brain it is also possible that deamidated PrP^{C} might arise via an enzymatic route (80).

It has been argued that deamidation and racemization of asparagine residues do not comprise a crucial or obligatory determinant in formation of PrP^{Sc} in rapid models of experimental scrapie disease, as stoichiometric elevations of altered aspartyl residues are absent from corresponding PrP^{Sc} preparations (35). Thus, most likely, our findings do not address the fundamental mechanism of prion replication as it occurs in experimental prion disease. However, we believe our data may speak to two other issues in the realm of prion pathobiology. The first issue is that of sporadic prion disease. We strongly suggest that abnormal PrP species arising by an interaction between deamidated forms of PrP^{C} and Cu(II) may engender or serve as precursors to the prions that underlie sporadic prion disease. The second issue is a potential relationship between deamidation and prion strains.

The residue C-terminal to Asn is a potent determinant of deamidation rates *in vitro* and *in vivo* (53, 83–85). Remarkably, in the case of Asn-107, this is the site of a missense polymorphism (Leu-108 → Phe-108) that may control susceptibility to prion strains (18, 21). Thus comparative studies of deamidation rates in Leu-108 and Phe-108 variants of PrP^{C} would seem warranted. Furthermore, as Asn deamidation can generate six covalent variants in addition to the "parental" L-Asn residue (86)) and 5–8 prion strains can be identified in a given inbred host (16, 87), could these phenomena be related? In short, could covalent variants of the PrP backbone comprise strain determinants? Although it is established that PrP^{Sc} from rapidly replicating prion strains such as 263K and Sc237 includes L-Asn-107 (35, 88), more slowly replicating strains might encompass covalent derivatives of Asn-107 generated by rate-

limiting deamidative pathways. Although these notions are currently speculative, our findings suggest that experiments to catalogue Asn derivatives in brain PrP and to create mutations at or in the vicinity of codon 107 may provide new insights into prion disease pathogenesis.

Acknowledgments—We thank Peter Mastrangelo and Maria Gasset for helpful discussions and Lynle Go and Bob Strome for technical assistance. We also thank R. Glockshuber, S. Hornemann, and M. Cereghetti for gifts of recombinant MoPrP23-231 and discussions of unpublished results; R. Rubenstein for 3F4 antibody, and the Biotechnology Service Center, Department of Clinical Biochemistry, University of Toronto for peptide sequencing.

REFERENCES

1. Prusiner, S. B. (1998) *Proc. Natl. Acad. Sci. U. S. A.* **95,** 13363–13383
2. Borchelt, D. R., Scott, M., Taraboulos, A., Stahl, N., and Prusiner, S. B. (1990) *J. Cell Biol.* **110,** 743–752
3. Caughey, B., and Raymond, G. J. (1991) *J. Biol. Chem.* **266,** 18217–18223
4. Gasset, M., Baldwin, M. A., Fletterick, R. J., and Prusiner, S. B. (1993) *Proc. Natl. Acad. Sci. U. S. A.* **90,** 1–5
5. Pan, K.-M., Baldwin, M., Nguyen, J., Gasset, M., Serban, A., Groth, D., Mehlhorn, I., Huang, Z., Fletterick, R. J., Cohen, F. E., and Prusiner, S. B. (1993) *Proc. Natl. Acad. Sci. U. S. A.* **90,** 10962–10966
6. McKinley, M. P., Bolton, D. C., and Prusiner, S. B. (1983) *Cell* **35,** 57–62
7. Oesch, B., Westaway, D., Wälchli, M., McKinley, M. P., Kent, S. B. H., Aebersold, R., Barry, R. A., Tempst, P., Teplow, D. B., Hood, L. E., Prusiner, S. B., and Weissmann, C. (1985) *Cell* **40,** 735–746
8. Westaway, D., Carlson, G. A., and Prusiner, S. B. (1989) *Trends Neurosci.* **12,** 221–227
9. Gibbs, C. J., Jr., Gajdusek, D. C., and Amyx, H. (1979) in *Slow Transmissible Diseases of the Nervous System* (Prusiner, S. B., and Hadlow, W. J., eds) Vol. 2, pp. 87–110, Academic Press, New York
10. Parchi, P., Giese, A., Capellari, S., Brown, P., Schulz-Schaeffer, W., Windl, O., Zerr, I., Budka, H., Kopp, N., Piccardo, P., Poser, S., Rojiani, A., Streichemberger, N., Julien, J., Vital, C., Ghetti, B., Gambetti, P., and Kretzschmar, H. (1999) *Ann. Neurol.* **46,** 224–233
11. Bruce, M. E. (1993) *Br. Med. Bull.* **49,** 822–838
12. Kimberlin, R. H., Walker, C. A., and Fraser, H. (1989) *J. Gen. Virol.* **70,** 2017–2025
13. Kellings, K., Prusiner, S. B., and Riesner, D. (1994) *Philos. Trans. R. Soc. Lond-Biol. Sci.* **343,** 425–430
14. Bessen, R. A., and Marsh, R. F. (1994) *J. Virol.* **68,** 7859–7868
15. Telling, G. C., Parchi, P., DeArmond, S. J., Cortelli, P., Montagna, P., Gabizon, R., Mastriani, J., Lugaresi, E., Gambetti, P., and Prusiner, S. B. (1996) *Science* **274,** 2079–2082
16. Safar, J., Wille, H., Itri, V., Groth, D., Serban, H., Torchia, M., Cohen, F. E., and Prusiner, S. B. (1998) *Nat. Med.* **4,** 1157–1165
17. Kanyo, Z. F., Pan, K. M., Williamson, R. A., Burton, D. R., Prusiner, S. B., Fletterick, R. J., and Cohen, F. E. (1999) *J. Mol. Biol.* **293,** 855–863
18. Westaway, D., Goodman, P. A., Mirenda, C. A., McKinley, M. P., Carlson, G. A., and Prusiner, S. B. (1987) *Cell* **51,** 651–662
19. Hunter, N., Hope, J., McConnell, I., and Dickinson, A. G. (1987) *J. Gen. Virol.* **68,** 2711–2716
20. Carlson, G. A., Goodman, P. A., Lovett, M., Taylor, B. A., Marshall, S. T., Peterson-Torchia, M., Westaway, D., and Prusiner, S. B. (1988) *Mol. Cell. Biol.* **8,** 5528–5540
21. Moore, R. C., Hope, J., McBride, P. A., McConnell, I., Selfridge, J., Melton, D. W., and Manson, J. C. (1998) *Nat. Genet.* **18,** 118–125
22. DeArmond, S. J., McKinley, M. P., Barry, R. A., Braunfeld, M. B., McColloch, J. R., and Prusiner, S. B. (1985) *Cell* **41,** 221–235
23. Sulkowski, E. (1992) *FEBS Lett.* **307,** 129–130
24. Hornshaw, M. P., McDermott, J. R., and Candy, J. M. (1995) *Biochem. Biophys. Res. Commun.* **207,** 621–629
25. Brown, D. R., Qin, K., Herms, J., Madlung, A., von Bohlen, A., Manson, J., Strome, R., Fraser, P. E., Kruck, T., Schulz-Schaeffer, W., Giese, A., Westaway, D., and Kretzschmar, H. A. (1997) *Nature* **390,** 684–687
26. Stockel, J., Safar, J., Wallace, A. C., Cohen, F. E., and Prusiner, S. B. (1998) *Biochemistry* **37,** 7185–7193
27. Viles, J. H., Cohen, F. E., Prusiner, S. B., Goodin, D. B., Wright, P. E., and Dyson, H. J. (1999) *Proc. Natl. Acad. Sci. U. S. A.* **96,** 2042–2047
28. Herms, J., Tings, T., Gall, S., Madlung, A., Giese, A., Siebert, H., Schurmann, P., Windl, O., Brose, N., and Kretzschmar, H. (1999) *J. Neurosci.* **19,** 8866–8875
29. Brown, D. R., Schulz-Schaeffer, B., Schmidt, B., and Krtezschmar, H. A. (1997) *Exp. Neurol.* **146,** 104–112
30. Shaked, Y., Rosenmann, H., Talmor, G., and Gabizon, R. (1999) *J. Biol. Chem.* **274,** 32153–32158
31. Brown, D. R., Wong, B. S., Hafiz, F., Clive, C., Haswell, S. J., and Jones, I. M. (1999) *Biochem. J.* **344,** 1–5
32. Wadsworth, J. D. F., Hill, A. F., Joiner, S., Jackson, G. S., Clarke, A. R., and Collinge, J. (1999) *Nat. Cell Biol.* **1,** 55–59
33. Hornemann, S., Korth, C., Oesch, B., Riek, R., Wider, G., Wuthrich, K., and Glockshuber, R. (1997) *FEBS Lett.* **413,** 277–281
34. Sandmeier, E., Hunziker, P., Kunz, B., Sack, R., and Christen, P. (1999) *Biochem. Biophys. Res. Commun.* **261,** 578–583
35. Weber, D. J., McFadden, P. N., and Caughey, B. (1998) *Biochem. Biophys. Res. Commun.* **246,** 606–608
36. Prusiner, S. B., Scott, M., Foster, D., Pan, K.-M., Groth, D., Mirenda, C., Torchia, M., Yang, S.-L., Serban, D., Carlson, G. A., Hoppe, P. C., Westaway, D., and DeArmond, S. J. (1990) *Cell* **63,** 673–686
37. Meyer, R. K., McKinley, M. P., Bowman, K. A., Braunfeld, M. B., Barry, R. A., and Prusiner, S. B. (1986) *Proc. Natl. Acad. Sci. U. S. A.* **83,** 2310–2314
38. Hornshaw, M. P., McDermott, J. R., Candy, J. M., and Lakey, J. H. (1995) *Biochem. Biophys. Res. Commun.* **214,** 993–999
39. Miura, T., Hori-i, A., and Takeuchi, H. (1996) *FEBS Lett.* **396,** 248–252
40. Riek, R., Hornemann, S., Wider, G., Glockshuber, R., and Wuthrich, K. (1997) *FEBS Lett.* **413,** 282–288
41. Donne, D. G., Viles, J. H., Groth, D., Mehlhorn, I., James, T. L., Cohen, F. E., Prusiner, S. B., Wright, P. E., and Dyson, H. J. (1997) *Proc. Natl. Acad. Sci. U. S. A.* **94,** 13452–13457
42. Andrade, M. A., Chacon, P., Merelo, J. J., and Moran, F. (1993) *Protein Eng.* **6,** 383–390
43. Greenfield, N., and Fasman, G. D. (1969) *Biochemistry* **8,** 4108–4116
44. Locht, C., Chesebro, B., Race, R., and Keith, J. M. (1986) *Proc. Natl. Acad. Sci. U. S. A.* **83,** 6372–6376
45. Negro, A., De Filippis, V., Skaper, S. D., James, P., and Sorgato, M. C. (1997) *FEBS Lett.* **412,** 359–364
46. Marcotte, E. M., and Eisenberg, D. (1999) *Biochemistry* **38,** 667–676
47. Maeda, H. (1997) *Langmuir* **13,** 4150–4161
48. Lau, S. J., and Sarkar, B. (1971) *J. Biol. Chem.* **246,** 5938–5943
49. Harris, D. A., Huber, M. T., van Dijken, P., Shyng, S.-L., Chait, B. T., and Wang, R. (1993) *Biochemistry* **32,** 1009–1016
50. Merz, P. A., Somerville, R. A., Wisniewski, H. M., and Iqbal, K. (1981) *Acta Neuropathol.* **54,** 63–74
51. McKinley, M. P., Braunfeld, M. B., and Prusiner, S. B. (1987) in *Prions: Novel Infectious Pathogens Causing Scrapie and Creutzfeldt-Jakob Disease* (Prusiner, S. B., and McKinley, M. P., eds) pp. 197–237, Academic Press, Orlando
52. Wong, B. S., Wang, H., Brown, D. R., and Jones, I. M. (1999) *Biochem. Biophys. Res. Commun.* **259,** 352–355
53. Brennan, T. V., and Clarke, S. (1995) in *Deamidation and Isoaspartate Formation in Peptides and Proteins* (Aswad, D. W., ed) pp. 66–90, CRC Press, Inc., Boca Raton, FL
54. Chen, S. G., Teplow, D., Parchi, P., Gambetti, P., and Autilio-Gambetti, L. (1995) *J. Biol. Chem.* **270,** 19173–19180
55. Kascsak, R. J., Rubenstein, R., Merz, P. A., Tonna-DeMasi, M., Fersko, R., Carp, R. I., Wisniewski, H. M., and Diringer, H. (1987) *J. Virol.* **61,** 3688–3693
56. Korth, C., Stierli, B., Streit, P., Moser, M., Schaller, O., Fischer, R., Schulz-Schaeffer, W., Kretzschmar, H., Raeber, A., Braun, U., Ehrensperger, F., Hornemann, S., Glockshuber, R., Riek, R., Billeter, M., and Oesch, B. (1997) *Nature* **390,** 74–77
57. Rogers, M., Taraboulos, A., Scott, M., Groth, D., and Prusiner, S. B. (1990) *Glycobiology* **1,** 101–109
58. Taraboulos, A., Rogers, M., Borchelt, D. R., McKinley, M. P., Scott, M., Serban, D., and Prusiner, S. B. (1990) *Proc. Natl. Acad. Sci. U. S. A.* **87,** 8262–8266
59. Hornemann, S., and Glockshuber, R. (1998) *Proc. Natl. Acad. Sci. U. S. A.* **95,** 6010–6014
60. Jackson, G. S., Hosszu, L. L., Power, A., Hill, A. F., Kenney, J., Saibil, H., Craven, C. J., Waltho, J. P., Clarke, A. R., and Collinge, J. (1999) *Science* **283,** 1935–1937
61. Kocisko, D. A., Come, J. H., Priola, S. A., Chesebro, B., Raymond, G. J., Lansbury, P. T., Jr., and Caughey, B. (1994) *Nature* **370,** 471–474
62. Bessen, R. A., Kocisko, D. A., Raymond, G. J., Nandan, S., Lansbury, P. T., and Caughey, B. (1995) *Nature* **375,** 698–700
63. Horiuchi, M., and Caughey, B. (1999) *EMBO J.* **18,** 3193–3203
64. Ma, J., and Lindquist, S. (1999) *Nat. Cell Biol.* **1,** 358–361
65. Capellari, S., Zaidi, S. I. A., Urig, C. B., Perry, G., Smith, M. A., and Petersen, R. B. (1999) *J. Biol. Chem.* **274,** 34846–34850
66. Paik, S. R., Shin, H. J., Lee, J. H., Chang, C. S., and Kim, J. (1999) *Biochem. J.* **340,** 821–828
67. Mehlhorn, I., Groth, D., Stockel, J., Moffat, B., Reilly, D., Yansura, D., Willett, W. S., Baldwin, M., Fletterick, R., Cohen, F. E., Vandlen, R., Henner, D., and Prusiner, S. B. (1996) *Biochemistry* **35,** 5528–5537
68. Li, S., Nguyen, T. H., Schoneich, C., and Borchardt, R. T. (1995) *Biochemistry* **34,** 5762–5772
69. Wright, H. T. (1991) *Protein Eng.* **4,** 283–294
70. Wright, H. T. (1991) *Crit. Rev. Biochem. Mol. Biol.* **26,** 1–52
71. Clarke, S., Stephenson, R. C., and Lowenson, J. L. (1992) *Stability of Protein Pharmaceuticals* (Ahern, T. J., and Manning, M. C., eds) pp. 1–29, Plenum Publishing Corp., New York
72. Xie, M., and Schowen, R. L. (1999) *J. Pharmacol. Sci.* **88,** 8–13
73. Gabriel, J.-M., Oesch, B., Kretzschmar, H., Scott, M., and Prusiner, S. B. (1992) *Proc. Natl. Acad. Sci. U. S. A.* **89,** 9097–9101
74. Peretz, D., Williamson, R. A., Matsunaga, Y., Serban, H., Pinilla, C., Bastidas, R. B., Rozenshteyn, R., James, T. L., Houghten, R. A., Cohen, F. E., Prusiber, S. B., and Burton, D. R. (1997) *J. Mol. Biol.* **273,** 614–622
75. Hedge, R. S., Mastrianni, J. A., Scott, M. R., DeFea, K. A., Trembaly, P., Orchia, M., DeArmond, S. J., Prusiner, S. B., and Lingappa, V. R. (1998) *Science* **279,** 827–834
76. Takemoto, L. J. (1995) in *Deamidation and Isoaspartate Formation in Peptides and Proteins* (Aswad, D. W., ed) pp. 157–165, CRC Press, Inc., Boca Raton, FL
77. Paleari, R., Paglietti, E., Mosca, A., Mortarino, M., Maccioni, L., Satta, S., Cao, A., and Galanello, R. (1999) *Clin. Chem.* **45,** 21–28
78. Watanabe, A., Takio, K., and Ihara, Y. (1999) *J. Biol. Chem.* **274,** 7368–7378
79. McIntire, W. E., Schey, K. L., Knapp, D. R., and Hildebrandt, J. D. (1998) *Biochemistry* **37,** 14651–14658
80. Exner, T., Jensen, O. N., Mann, M., Kleuss, C., and Nurnberg, B. (1999) *Proc. Natl. Acad. Sci. U. S. A.* **96,** 1327–1332
81. McFadden, P. N., and Clarke, S. (1982) *Proc. Natl. Acad. Sci. U. S. A.* **79,** 2460–2464

82. Potter, S. M., Johnson, B. A., Henschen, A., Aswad, D. W., and Guzzetta, A. W. (1992) *Biochemistry* **31,** 6339–6347
83. Johnson, B. A., and Aswad, D. W. (1995) in *Deamidation and Isoaspartate Formation in Peptides and Proteins* (Aswad, D. W., ed) pp. 91–113, CRC Press, Inc., Boca Raton, FL
84. Blackwell, R. Q., Boon, W. H., Liu, C. S., and Weng, M. I. (1972) *Biochim. Biophys. Acta* **278,** 482–490
85. Wajcman, H., Kister, J., Vasseur, C., Blouquit, Y., Trastour, J. C., Cottenceau, D., and Galacteros, F. (1992) *Biochim. Biophys. Acta* **1138,** 127–132
86. Geiger, T., and Clarke, S. (1987) *J. Biol. Chem.* **262,** 785–794
87. Bruce, M. E. (1996) in *Prion Diseases* (Baker, H. F., and Ridley, R. M., eds) pp. 223–236, Humana Press Inc., Totawa, NJ
88. Stahl, N., Baldwin, M. A., Teplow, D. B., Hood, L., Gibson, B. W., Burlingame, A. L., and Prusiner, S. B. (1993) *Biochemistry* **32,** 1991–2002